Preparation and Evaluation of Weldments Employing the Rotary Arc GMA-NG Process

by

B.M. Patchett

University of Alberta

Work on this project was conducted under the auspices of the Canada Centre for Mineral and Energy Technology, Energy, Mines and Resources, Canada.

DSS File Number: 52SS. 23440 - 6 - 9142

Contract Serial Number: 23440 - 6 - 9142 / 01-ST

CANMET Scientific Authority: Dr. J.T. McGrath

21 pp

MICROMEDIA

90-03958/

MICROSTRUCTURE AND MECHANICAL PROPERTIES OF ROTARY ARC GMA-NG WELDS IN HSLA80 AND HY100 STEELS

by

B.M. PATCHETT*, A. C. BICKNELL*, N.J.G. SMITH** and J.A. GIANETTO**

*University of Alberta

**Metals Technology Laboratories

CANMET

OTTAWA, CANADA

ABSTRACT

One-sided welds were produced in 25 mm thick precipitation hardened HSLA80 and quenched and tempered HY100 steels using a rotary arc single pass/layer narrow gap welding technique at a nominal energy input of 2 kJ/mm. Three welds were produced and evaluated according to the military standards for submarine construction. One weld was produced in HSLA80 steel using a commercially available 100S-1 electrode wire. Two welds were produced in HY100 steel, one using the same commercially available 100S-1 wire and one using a commercially available 120S-1 wire, in combination with a 95%Ar-5%CO2 shielding gas mixture.

The results showed that the specified combination of weld metal strength (≥565 MPa) and notch toughness (47J at -51°C and 81J at -18°C) was obtained for the weld made in the HSLA80 steel. The weld made in the HY100 steel with the 100S-1 wire also exceeded the targeted notch toughness. However, the yield strength was marginally low (670 MPa compared with the target of 703 MPa). The weld made in the HY100 steel with the 120S-1 wire had a very high weld metal yield strength (817 MPa) and marginally low notch toughness (45J at -51°C).

The superior notch toughness of the weld made in the HSLA80 was attributed to a microstructure consisting of a high proportion of acicular ferrite and some discontinuous grain boundary ferrite. A comparison of the two HY100 welds showed that the lower strength of the HY100 weld metal made with the 100S-1 wire was associated with improved notch toughness compared with the HY100 weld made with the 120S-1 wire. The latter weld had a very high yield strength resulting from the more highly alloyed weld deposit, which transformed to a mixture of martensitic and bainitic (ferrite with second phase) transformation products.

MICROSTRUCTURE ET PROPRIÉTÉS MÉCANIQUES DE SOUDURE RÉALISÉES A L'ARC TOURNANT SOUS PROTECTION GAZEUSE AVEC FAIBLE ÉCARTEMENT DANS DES ACIERS HSLA80 ET HY100

B.M. PATCHETT*, A. C. BICKNELL*, N.J.G. SMITH** and J.A. GIANETTO**

*University of Alberta
**Laboratoires de la technologie des métaux
CANMET
OTTAWA, CANADA

RESUME

Des soudures d'un seul côté ont été réalisées sur des aciers HY100 trempés et revenus et des aciers HSLA80 durcis par précipitation de 25 mm d'épaisseur par une technique de soudage à l'arc tournant, à une seule passe/couche, avec faible écartement, à un apport d'énergie nominal de 2 kJ/mm. Trois soudures ont été réalisées et évaluées conformément aux normes militaires applicables à la construction des sous-marins. Une des soudures a été réalisée sur de l'acier HSLA80 à l'aide d'un fil-électrode 100S-1 disponible sur le marché Les deux autres on été réalisées sur de l'acier HY100, l'une avec le fil-électrode 100S-1, l'autre avec un autre type de fil-électrode disponible sur le marché, le 120S-1, avec un mélange de gaz inerte composé de 95 % d"Ar et 5 % de CO2.

Les résultats ont montré qu'on obtenait une excellente combinaision de la limite conventionnelle de proportionnalité du métal de soudure (≥565 MPa) et de la résistance à l'entaille (47J a -51°C et 81J a -18°C) dans le cas de la soudure produite sur l'acier HSLA80. Dans le cas de la soudure produite sur l'acier HY100 avec l'électrode 100S-1, la résistance à l'entaille dépassait la valeur visée mais la limite conventionnelle de proportionnalité était un peu faible (670 MPa comparativement à une valeur visée de 703 MPa). Quant à la soudure réalisée sur l'acier HY100 avec l'électrode 120S-1, la limite conventionnelle de proportionnalité du metal de soudure était très élevée (817 MPa) et la résistance à l'entaille un peu faible (45J a -51°C).

La plus grande résistance à l'entaille obtenue dans le cas de la soudure réalisée sur l'acier HSLA80 a été attribuée à une microstructure composée d'une grande partie de ferrite aciculaire et d'un peu de ferrite intergranulaire discontinue. Une comparaison des deux soudures réalisées sur l'acier HY100 a montré que la plus faible limite conventionnelle de proportionnalité obtenue avec l'électrode 100S-1 se traduisait par une résistance à l'entaille plus grande que celle obtenue avec l'électrode 120S-1. La soudure produite avec l'électrode 120S-1 présentait une limite conventionnelle de proportionnalité très élevée attribuable au métal de soudure plus fortement allié qui s'est transformé en un mélange de produits martensitiques et bainitiques (ferrite avec deuxième phase).

INTRODUCTION

The objective of the present study was to evaluate the rotary gas-metal-arc narrow gap welding process for the fabrication of weldments in high strength steels which would meet the military standards for naval vessels. For this study, welds were produced in both 25 mm thick HSLA80 and HY100 steels, using a one-sided welding technique and two commercially available electrode wires.

Previous studies (Ref. 1, 2) have shown that the rotary arc single pass/layer narrow gap welding technique can produce economic savings because it can have faster joint completion rates and lower distortion than conventional groove welds, with superior mechanical properties. Another potential advantage for shipyard fabrication is that it can be used to produce one-sided welds.

Offsetting these potential advantages are the additional costs associated with fit-up, since the narrow gap technique requires tighter tolerances than conventional groove welds. Because of these additional costs, narrow gap welding procedures are usually only economical for welding thick section components. However, welding processes for high strength steels, particularly for military applications, are rarely operated at their full economic potential because of the difficulty of achieving the combination of high yield strength and high toughness required by the military specifications. The cost of producing high strength steel welds for naval vessels, particularly submarines, is high and it is difficult to achieve the target mechanical properties (Ref. 3, 4, 5). Therefore, the rotary arc technique has potential advantages and could prove economical for welding high-strength steels. The present investigation was performed to evaluate the potential of the rotary-arc narrow gap process for joining HSLA80 and HY100 steels. The mechanical property requirements used in this report are in accordance with the military standard for GMAW consumable qualification of HY80/100 (Ref. 6) and are presented in Table 1.

The NKK rotary arc GMAW system was developed within the last decade to ensure excellent side-wall fusion in monopass narrow-gap welds by increasing the oscillatory frequency of the single electrode arc welding process (Ref. 1). The electrode is fed through a hollow guide tube into an eccentric outlet hole in the contact tip at the bottom of the tube. The tube is rotated by an electric motor to produce the rotary motion, which ensures simultaneous fusion of the side walls of the joint. Lack of fusion flaws were the major cause of weld rejection in early work on narrow gap procedures. The maximum rotational frequency is 150 Hz on a rotational diameter for the electrode wire of about 7 mm. The power is supplied by a Mitsubishi transistorized constant potential power source (500 A capacity) and the equipment includes automatic seam tracking and arc length control mechanisms. These function by reading the arc voltage and current at the front and rear of the weld pool (for arc length control) and at the closest approach to the two sidewall positions (for seam tracking). Electronic comparison of the voltages and currents is used to supply feedback control of

arc length and arc centralization in the joint gap. The overall schematic of the process for butt welding is shown in Figure 1.

EXPERIMENTAL

Materials and Welding Procedures

One-sided rotary arc single pass per layer narrow gap welds were produced in 25.4 mm thick HSLA80 and HY100 steels. The chemical compositions of the base materials are listed in Table 2. These base materials were produced in accordance with the respective military standards (Ref 6, 7).

The experimental rotary arc welds for this investigation were prepared using a one-sided welding technique. The preheat and interpass temperature limitations of the military standard were strictly observed. The completed welds were 1.2 m long by 0.6 m wide. The welds were made using two commercially available electrode wires at a nominal energy input of ~2 kJ/mm. The chemical composition of the electrodes are listed in Table 3. One weld was produced in HSLA80 using a 100S-1 electrode wire, and two welds were produced in HY100, one weld using the same 100S-1 electrode wire and the other using a 120S-1 electrode wire. A single 1.2 mm diameter electrode was employed. The welds were prepared with the welding consumables and parameters listed in Tables 4 and 5. The 95%Ar-5%CO_2 shielding gas was selected to minimize weld metal oxidation while providing acceptable arc characteristics. Lower levels of CO_2 did not run properly in the narrow gap due to excessive spatter at low arc voltages. Higher levels of CO_2 ran well, but the oxidation potential was considered to be too high for optimum high strength low alloy toughness. A narrow gap joint design with a gap of 13 mm and a 1.5 mm root face was selected after some preliminary trials. The trials showed that welding procedures utilizing an open root and a metallic backing bar did not provide good root fusion for low alloy steels. Welding with a machined root face without backing of any kind caused unacceptable oxidation of the root pass and occasional excessive penetration. Therefore, a ceramic backing, 3M-SJ8074, was used as a temporary backing for the final "production" welds. The joint design and the macrosection for the single-pass per layer welds are shown in Figures 2 and 3. Each completed weld was inspected by X-ray radiography before machining the mechanical test specimens.

Mechanical Testing and Metallography

Tensile, CVN, and microhardness tests were performed on each weldment to characterize the effects of different welding consumables. For the weld metal, the tensile properties were determined from all-weld-metal tensile specimens machined from the sub-surface region of the weld joints. Charpy V-notch specimens were machined transverse to the weld length and notched

through-thickness at the weld centreline. The CVN specimens were taken 2 mm below the original plate surface. Testing was performed at temperatures between -80°C and 20°C. The key test temperatures (-50°C and -20°C) were selected from the military standard for consumable qualification of submerged-arc welding consumables for HY80/100 (Ref. 6).

The microstructure of the weld metal was characterized by optical microscopy on sections prepared by standard metallographic techniques. The microstructural constituents were identified by optical microscope according to the IIW guidelines (Ref. 8). The proportion of as-deposited and reheated weld metal regions was determined for the Charpy locations at the weld centreline.

Microhardness measurements were made in the vicinity of the Charpy notch locations at the weld metal centreline to further characterize the microstructure using a diamond pyramid indenter with a 500 g load.

RESULTS

Visual inspection of the welds showed that excellent bead shape was obtained with minimal undercut. The ceramic backing selected for this investigation performed well, with no excessive root penetration observed. X-ray radiography of the completed welds did not reveal any cracks or unacceptable porosity.

Weld Metal Chemistry

The weld-metal chemical compositions of the three welds, BP82, BP102, and BP103, were determined for the sub-surface region. These chemical compositions are listed in Table 6. The weld metal compositions resulted primarily from the alloy additions in the electrode wire and some dilution from the respective base plates. For comparison, the chemical compositions of the corresponding base plates and electrode wires are listed in Tables 2 and 3, respectively. The hardenability of each of these weld metal compositions was calculated using the IIW carbon-equivalent formula. The results of these calculations, also shown in Table 6, indicate that the welds BP82 and BP102 had similar hardenability, while weld BP103 was more highly alloyed.

Both welds BP 82 (with the HSLA80 base plate) and BP102 (with the HY100 base plate) were made with the 100S-1 electrode wire. Only slight differences were observed between these two welds. In general, BP102 had higher levels of C and Cr and a lower level of Cu than BP82. These differences are caused by dilution with the base plate.

The welds BP102 (with the 100S-1 electrode wire) and BP103 (with the 120S-1 electrode wire) were made using the HY100 base plate. In general, the weld metal for BP103 was more highly alloyed, with higher C, Ni, Cr, and Mo levels and lower Cu and Si levels than BP102.

These differences arise from the chemical compositions of the electrode wires, since the same HY100 base plate was used.

Weld Metal Microstructure

Figure 3 shows representative macrosections of the rotary arc welds. The weld metal microstructure of the narrow gap welds, BP82, BP102, and BP103, in the location where both the tensile and CVN specimens were taken contained both as-deposited and reheated weld metal regions. A survey, taken at the centreline of the weld to determine the proportion of as-deposited and reheated structure, showed that the proportion of as-deposited structure was about 70% for all three welds.

Representative optical micrographs of the as-deposited region of BP82, BP102, and BP103 are shown in Figures 4, 5, and 6 respectively. Microhardness results for both the as-deposited and reheated regions are shown in Table 7.

The microstructure within the as-deposited region of BP82 was composed of a high proportion of acicular ferrite with some discontinuous grain boundary ferrite and ferrite with second phase. The presence of some martensite-austenite (M-A) micro-phase was observed between the acicular ferrite laths and at the prior austenite grain boundaries. The primary structure, that is the prior austenite grains, consisted of elongated columnar grains approximately 150 to 250 μm wide. In the reheated region, the primary structure consisted of prior austenite grain structures which ranged from polygonal shaped grains 30 to 40 μm in diameter to coarser, more elongated grains depending on the austenizing temperature and the time at temperature. The transformed structure in the reheated regions also consisted primarily of acicular ferrite, Figure 7a. There was a slight decrease in microhardness observed between the as-deposited and reheated regions.

The microstructure within the BP102 weld, made with the same 100S-1 electrode wire as BP82, was similar to the BP82 weld metal microstructure for both the as-deposited and reheated regions. This reflected the similarity in weld metal compositions. In general, the as-deposited region of BP102 had less grain boundary ferrite and ferrite with second phase structures than BP82. However, there was some indication of individual bainitic laths, with an aspect ratio of about 10:1, in BP102. The transformed structure in the reheated regions also consisted primarily of acicular ferrite, as shown in Figure 7b. The microhardness was slightly higher than weld BP82, reflecting the difference in weld metal chemistry.

The microstructure within the as-deposited region of BP103 was classified as martensite and bainite (ferrite with second phase) packets. The transformed structures in the reheated region were also similar to the as deposited in this weld, Figure 7c. This weld had the highest microhardness readings (~375 Hv), which corresponded to the more highly alloyed deposit (CE ~ 0.67).

Weld Metal Mechanical Properties

The tensile properties of the HSLA80 and HY100 welds were measured from all-weld metal tensile specimens. The results are presented in Table 8. The toughness of the weld metal was assessed by CVN tests (Table 1) and the results are presented in Table 9 and Figure 8. These CVN toughness results represent the average of three specimens per test temperature.

The evaluation of the mechanical properties of the HSLA80 weld deposit, BP82, showed that the weld metal notch toughness requirements (47 J at -50°C and 81 J at -18°C) and yield strength requirement of 565 MPa were achieved using commercially available 100S-1 electrode wire. The measured yield strength of BP82, 658 MPa, exceeded the specification yield strength requirement. The elongation and reduction in area requirements were also exceeded. This weld also exhibited good Charpy V notch toughness, exceeding the specification requirements, particularly at -50°C, with a measured impact energy of 103 J compared with a specification requirement of 47 J.

The evaluation of the mechanical properties of the two HY-100 weld deposits showed that the weld metal CVN requirements (47 J at -51°C and 81 J at -18°C) could also be achieved using the 100S-1 wire. However, the measured yield strength, 670 MPa, was slightly lower than the specification requirement of 703 MPa. This is related to the use of the 100S-1 electrode wire, nominally designed for HY-80 materials. The ultimate tensile strength (805 MPa), the elongation, and the reduction in area were satisfactory.

Weld BP103, the HY100 weld made using the 120S-1 electrode wire, exceeded the Charpy impact specification by a small margin at -20°C but was slightly low at -50°C (45 J compared to the specification requirement of 47 J). The measured yield strength, 817 MPa, was considerably higher than the specification requirement of 703 MPa. The ultimate strength was very high, 943 MPa. The elongation and the reduction in area exceeded the specification requirements.

DISCUSSION

The present study on narrow gap welding of HSLA80 and HY100 showed that the combination of high strength and high notch toughness required by the military specification for submarine construction can be achieved using the rotary arc narrow gap process with commercially available 100S-1 electrode in HSLA80 steel. However, the weld metal yield strength was low for the weld made in HY100 with the 100S-1 wire and extremely high for the weld made with the 120S-1 wire.

The combination of high strength and high notch toughness properties obtained in the weld metal can be explained on the basis of the weld metal composition and resulting microstructure, particularly the effective grain size.

In the HSLA80 weld metal (BP82), made with the 100S-1 electrode wire, the superior combination of strength and low temperature notch toughness was attributed to the high proportion of acicular ferrite. Acicular ferrite weld metals consist of highly dislocated, low aspect ratio (4:1) ferrite laths, typically 1 to 3 μm wide, separated by high angle grain boundaries. Acicular ferrite provides optimum resistance to cleavage crack propagation because the cracks must re-initiate at the closely spaced high-angle boundaries. In addition, the weld metal contained a small proportion of discontinuous grain boundary ferrite, which has been shown to be more resistant to cleavage crack propagation than welds containing long continuous grain boundary ferrite veins located at prior austenite grain boundaries (Ref. 9, 10).

In the HY100 weld metal made with the 100S-1 electrode wire (BP102), the good low temperature notch toughness was also attributed to the high proportion of acicular ferrite in the weld metal. The weld BP102 was only slightly stronger than BP82 (670 MPa compared with 658 MPa) and the most noticable difference to account for the drop in notch toughness was an increase in the proportion of ferrite with second phase (bainitic region) located throughout the weld metal structure. Thus, the overall resistance to cleavage crack propagation was lower since the effective grain size was considered to be slightly larger for weld BP102 than for weld BP82. Despite this observation, the weld BP102 exceeded the targeted notch toughness requirements.

In the HY100 weld metal made with the 120S-1 wire, BP103, the weld metal microstructure was classified as a mixture of low carbon martensite and bainite regions, reflected by the higher hardness than BP82 and BP102 (Table 7). Deb, Challenger, and Therrien (Ref 11) and Ablen et al (Ref 12), in previous studies, concluded from TEM examination that the structure of similar weld metals was composed of very fine ferrite laths of varying dimensions, corresponding to very fine martensitic and bainitic packets. The weld BP103 had a higher yield strength than the welds consisting of acicular ferrite microstructure observed in the previous welds. The measured yield strength, 817 MPa, actually exceeded the maximum specified in the military specification (703 to 785 MPa). However, the results of this investigation suggest that the inherently higher strength of the weld metal reduced the overall CVN toughness achieved, as shown in Figure 8. Although reasonable CVN toughness properties were obtained, a lower strength weld metal deposit may result in a better combination of properties.

In summary, the weld metals consisting of acicular ferrite microstructure had generally lower strengths and higher toughness properties than the weld metals consisting primarily of mixed martensite and bainite packets. The inherently high yield strength of weld BP103 limited the CVN toughness. It is recommended that consumables be selected to meet a yield strength of 700 to 725

MPa in order to improve the overall toughness. It is also recommended that future development of rotary arc narrow gap welding procedures for HY100 steel should include an evaluation of a 110S-1 class electrode wire.

CONCLUSIONS

1. The present study showed that a one-sided rotary arc single pass/layer narrow gap welding technique can produce sound welds in HSLA80 and HY100 steels, without post-weld hydrogen removal treatment.
2. An excellent combination of weld metal strength and toughness was obtained welding HSLA80 steel with a commercially available 100S-1 electrode wire at a nominal energy input of 2 kJ/mm. This was attributed to the high proportion of acicular ferrite combined with a small proportion of discontinuous grain boundary ferrite.
3. Acceptable weld metal notch toughness was obtained welding HY100 steel with commercially available 100S-1, however, the yield strength was marginally low. For the HY100 weld produced with the 120S-1 electrode wire the yield strength was extremely high and tended to limit the notch toughness obtained.

REFERENCES

1. Nomura, H.; Sugitani, Y. 1982. Narrow Gap MIG Welding Process with High Speed Rotating Arc. IIW Doc. XII-C-033-82.
2. Laing, B.; Heid, R.; Pollack, A. 1985. Narrow Gap Welding of HY100 Plate using closed loop, adaptive feedback, through-the-arc tracking technology. Welding Journal 64(11): 38.
3. Smith, N.J. 1988. A Review of Welding Processes for HY100 Submarine Hull Components. MTL 88-55(TR).
4. Montemarano, T.W.; Sack, B.P.; Gudas, J.P.; Vassilaros, M.G.; Vandervelt, H.H. 1986. High strength low alloy steels in naval construction. Journal of Ship Production 2 (3): 145-162.
5. Shackleton, D.N. 1973. Welding HY-100 and HY-130 Steels - a literature review. The Welding Institute. Abington: U.K.
6. U.S. Dept. of Defence 1983. Military Standard MIL-E-23765/2C (SH).
7. U.S. Dept. of Defence 1981. Military Standard MIL-STD-16216J (SH).
8. Pargeter, R.J.; Dolby, R.E. 1985. Guidelines for Classification of Ferritic Steel Weld Metal Microstructural Constituents Using the Light Microscope, IIW Doc. IX-1377-85.
9. Tweed, J.H.; Knott, J.F. 1987. Micromechanisms of Failure in C-Mn weld metals. Acta. Metall. 35(7): 1401-1414.
10. Gianetto, J.A.; Smith, N.J.G.; McGrath, J.T. 1989. Unpublished Research at MTL/CANMET.
11. Deb, P.; Challenger, K.D.; Therrien, A.E. 1987. Structure-property correlation of submerged-arc and gas-metal-arc weldments in HY-100 steel. Metallurgical Transactions A 18A(6):987-999.
12. Ablen, S.P.; Huppi, G.S.; Brown, E.L.; Matlock, D.K.; Edwards, G.R. 1987. The microstructure and properties of selected high strength ferritic weld metals. Proc. of the Eighteenth Annual Technical Meeting of the International Metallographic Society: 99-114. Columbus: IMS & Metals Park: ASM.

Table 1 Mechanical property requirements for HSLA80 and HY100 weldments.

Base Material	HSLA80	HY100
Yield Strength	565 MPa	703 MPa
Elongation	20 %	20%
Reduction of Area	50%	50%
Charpy Impact Energy	81 J @ -18°C 47 J @ -51°C	81 J @ -18°C 47 J @ -51°C

Table 2 Chemical composition of HSLA80 and HY100 steels.

Base Material	Element wt%										
	C	Mn	Si	S	P	Ni	Cr	Mo	Cu	Nb	CE
HY100	0.17	0.33	0.23	0.008	0.010	2.62	1.52	0.48	0.03	0.020	0.80
HSLA80	0.06	0.50	0.27	0.004	0.007	0.92	0.66	0.25	1.02	0.044	0.45

Note; CE IIW = C + Mn/6 + (Cr + Mo + V)/ 5 + (Ni + Cu)/ 15

Table 3. Chemical composition of gas-metal-arc welding electrode wires

Electrode Wire	Element wt%								
	C	Mn	Si	S	P	Ni	Cr	Mo	Cu
Linde 120	0.06	1.58	0.35	0.006	0.011	2.36	0.29	0.40	0.02
Lincoln LA100	0.07	1.57	0.52	0.004	0.004	1.86	0.03	0.28	0.06

Table 4. Welding consumables and identification codes

Series	Weld No	Energy Input kJ/mm	Consumables Wire/Shielding Gas
A	BP-82	2	Lincoln LA100/Ar-5%CO2
B	BP-102	2	Lincoln LA100/Ar-5%CO2
B	BP-103	2	Linde 120/Ar-5%CO2

Note: . Series A was made using HSLA80 base plate.

Series B were made using HY100 base plate.

Table 5. Gas-metal-arc welding parameters for HSLA80 and HY100 weldments.

Pass No	Energy Input (kJ/mm)	Current (A)	Travel Speed (mm/min)	Voltage (V)	Rotation ms/rev
1	0.75	200	400	24-25	-
2-5	2.0	350	290	29-30	20
6	2.0	350	290	31	20

Note: 1. Electrical Extension = 25 mm
2. Contact Tip Eccentricity = 2 mm
3. Preheat Temperature = 100 °C
4. Interpass Temperature = 120°C min 150°C max

Table 6 Chemical composition of GMA weld metals deposited in HSLA80 and HY100 steels.

Series	Weld No	Element wt%									
		C	Mn	Si	S	P	Ni	Cr	Mo	Cu	C.E.
A	BP82	0.05	1.40	0.42	0.007	0.005	1.70	0.11	0.36	0.22	0.51
B	BP102	0.07	1.40	0.42	0.008	0.005	1.80	0.26	0.40	0.09	0.56
B	BP103	0.08	1.40	0.33	0.011	0.013	2.20	0.50	0.48	0.01	0.67

Note: Al ≤ 0.020, Nb ≤ 0.010

Table 7. Microhardness data for weld metal regions in HSLA80 and HY100 steels.

Series	Weld No	Energy Input (kJ/mm)	As-Deposited Region	Reheated Region
A	BP82	2	264	255
B	BP102	2	272	268
B	BP103	2	326	325

Table 8 Tensile properties of GMAW metals deposited in HSLA80 and HY100 steels.

Series	Weld No	Energy Input (kJ/mm)	Yield Strength (MPa)	Ultimate Strength (MPa)	Elongation (%)	Reduction in Area (%)
A	BP82	2	658	768	28	75
B	BP102	2	670	775	27	70
B	BP103	2	817	927	25	65

Table 9 Charpy Impact Energy Data for GMAW Metals Deposited in HSLA80 and HY100 steels

Series	Weld No	Energy Input (kJ/mm)	Impact Energy, J	
			-50°C	-20°C
A	BP82	2	103	151
B	BP102	2	81	139
B	BP103	2	45	84

Figure 1. Schematic diagram of NKK rotary arc GMAW-NG system.

Figure 2. Schematic diagram showing joint design of experimental rotary arc narrow gap welds.

Figure 3. Representative macrosections of rotary arc narrow gap welds showing bead profiles and root bead configuration. (a) BP82 (b) BP102 (c) BP103.

Figure 4. Microstructure of as-deposited region in the final cap pass of weld BP82, showing acicular ferrite (AF), discontinuous grain boundary ferrite (GF), and ferrite with second phase (FS)

Figure 5. Microstructure of as-deposited region in the final cap pass of weld BP102, showing the acicular ferrite (AF), discontinuous grain boundary ferrite (GF), and ferrite with second phase (FS).

Figure 6. Microstructure of the as-deposited region in the final cap pass of weld BP103, showing the bainite and martensite packets.

Figure 7. Microstructure of the reheated regions of the experimental rotary arc welds. (a) weld BP82
(b) weld BP102 (c) weld BP103.

Figure 8. Charpy transition curves for experimental rotary arc welds

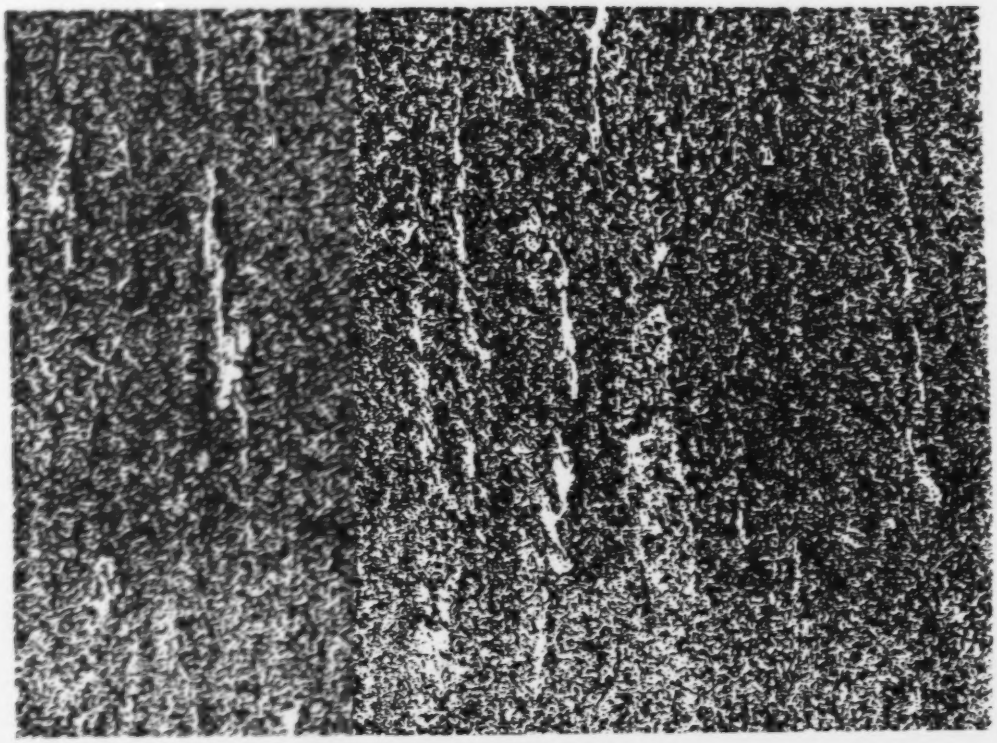

(a) Columnar structure

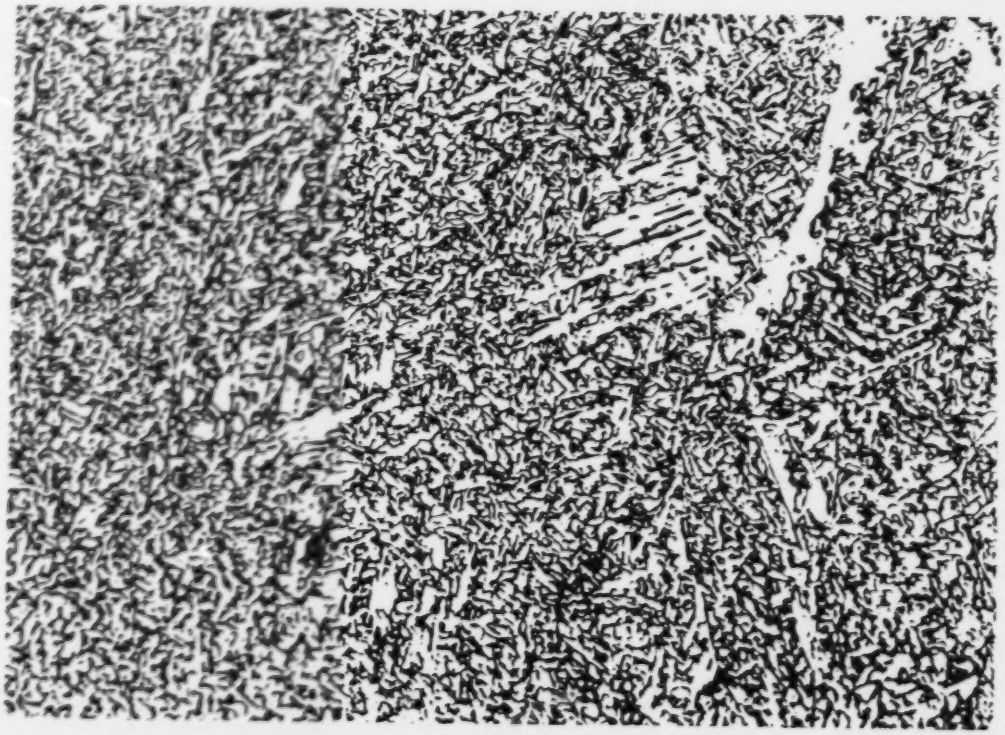

(b) Microstructural constituents

Fig. 3. Microstructure of as-deposited region in the final cap pass of weld BP82, showing acicular ferrite (AF), discontinuous grain boundary ferrite (GF), and ferrite with second phase (FS).

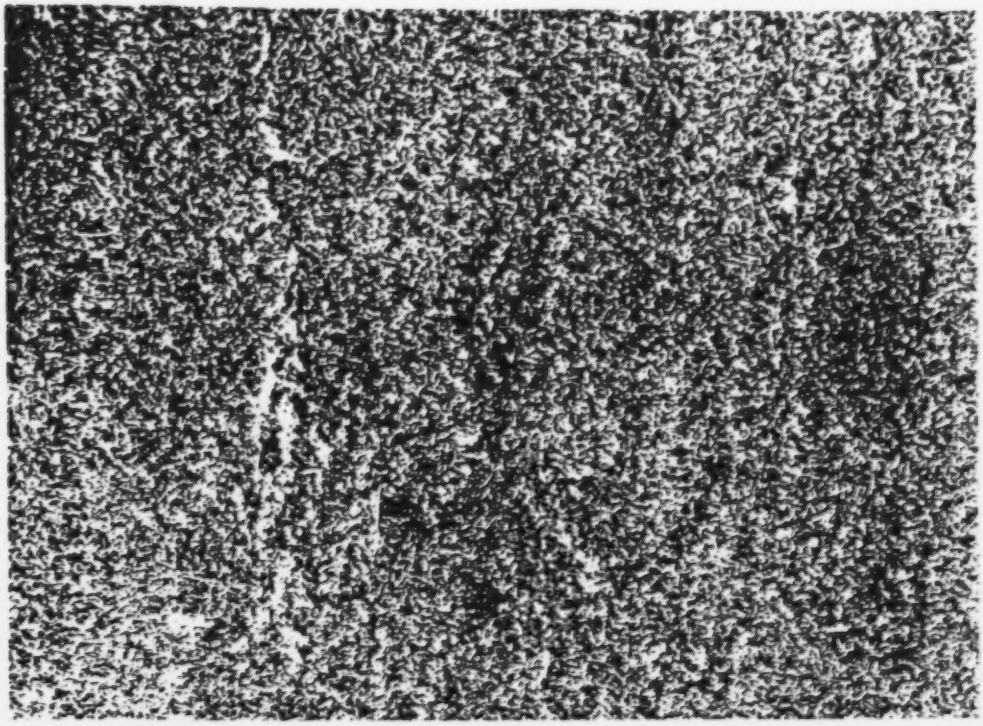

(a) Columnar structure

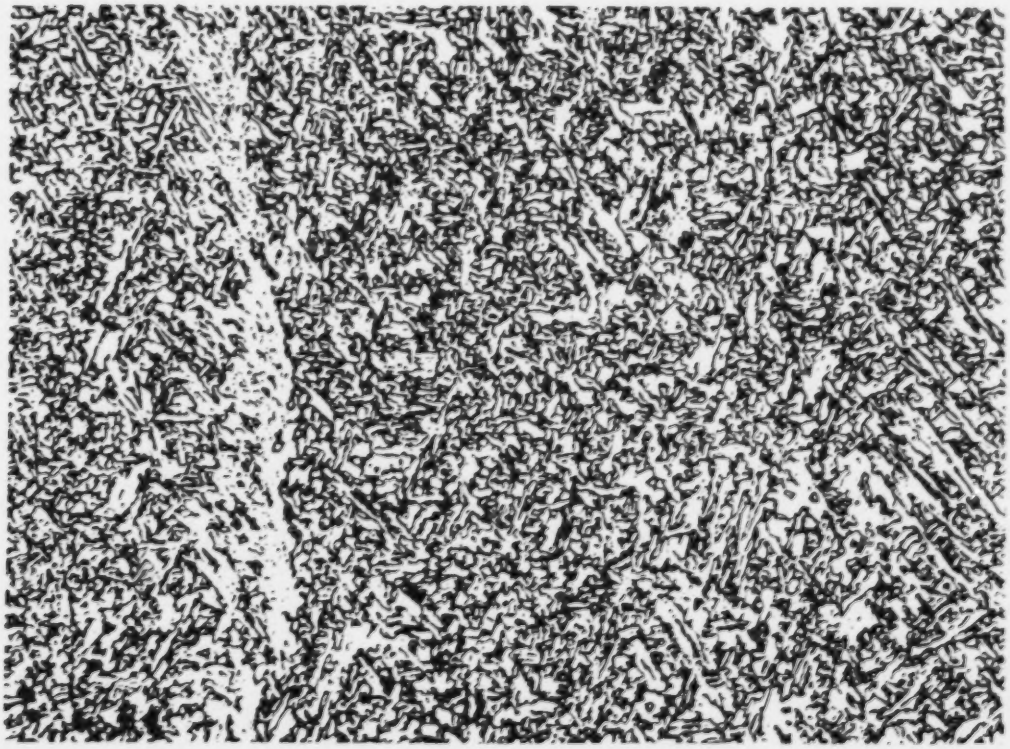

(b) Microstructural constituents

Fig. 4. Microstructure of as-deposited region in the final cap pass of weld BP102, showing the acicular ferrite (AF), discontinuous grain boundary ferrite (GF), and ferrite with second phase (FS).

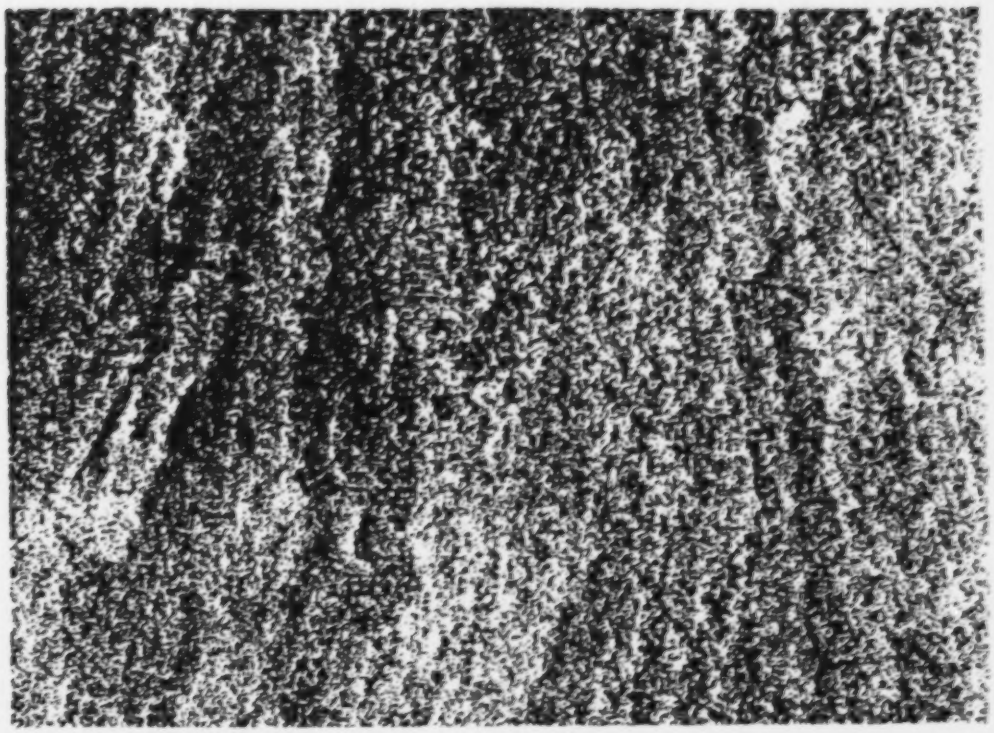

(a) Columnar structure

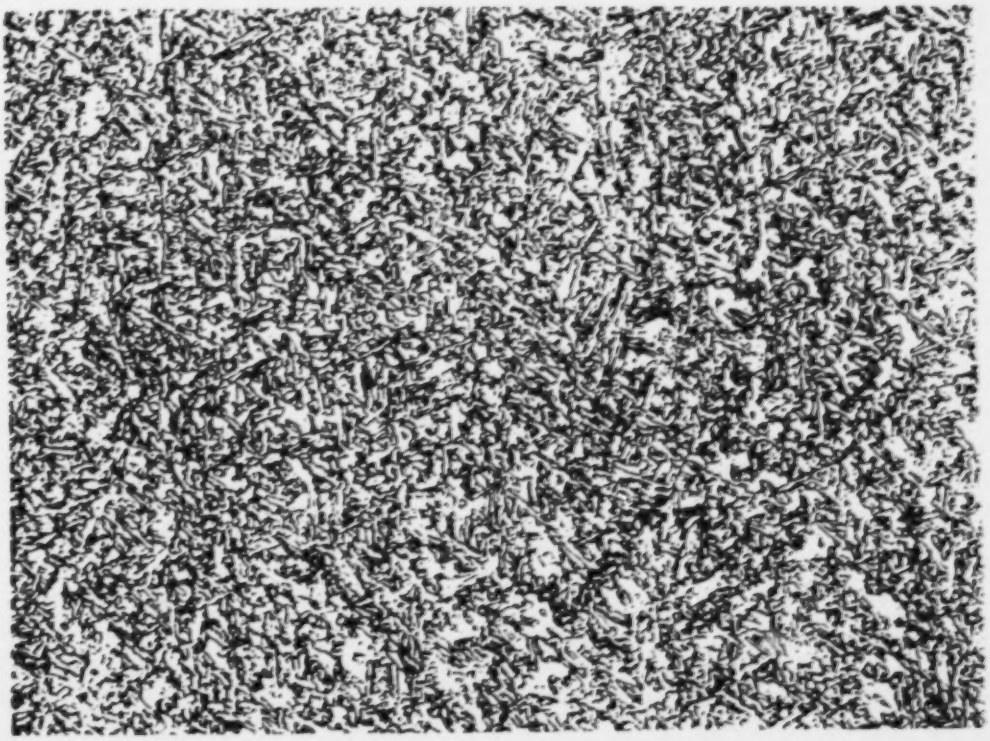

(b) Microstructural constituents

Fig. 5. Microstructure of the as-deposited region in the final cap pass of weld BP103, showing the bainite and martensite packets.

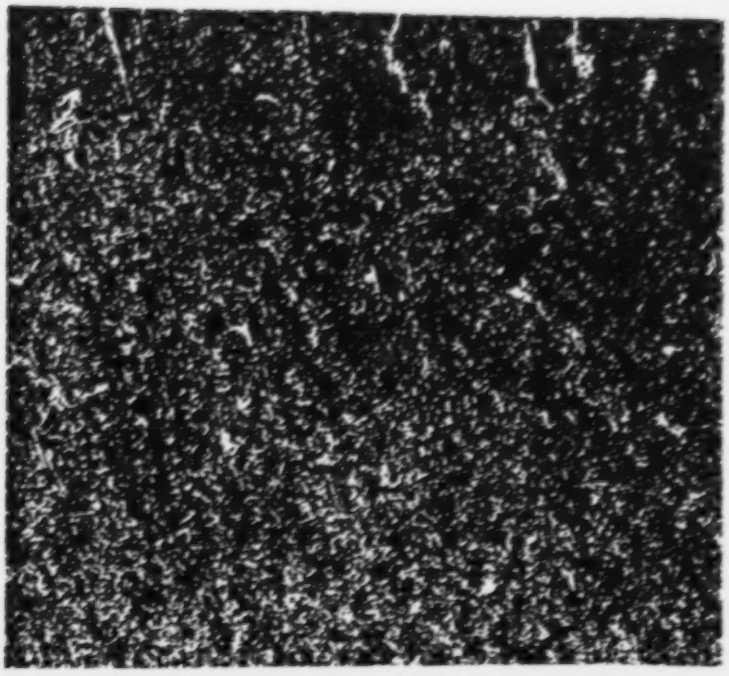

(a) Transition between as-deposited and reheated weld metal regions.

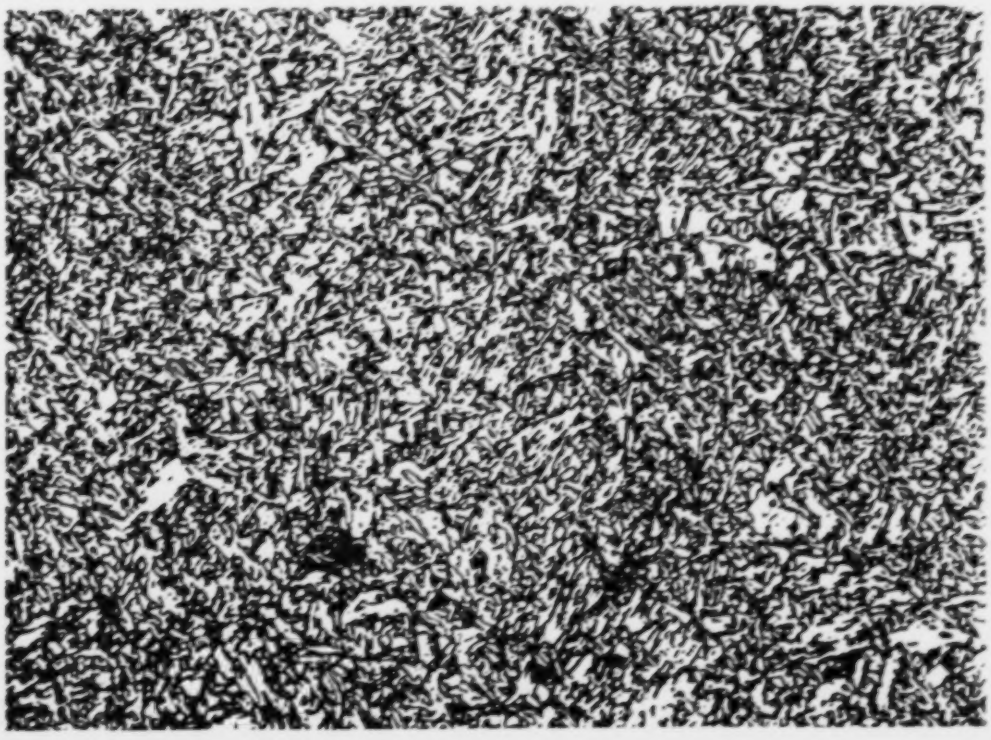

(b) Microstructural constituents

Fig. 6. Microstructure of the reheated regions of the experimental rotary arc narrow gap welds, (a) and (b) weld BP82, (c) weld BP102 and (d) weld BP103.

Fig. 6 Cont'd.

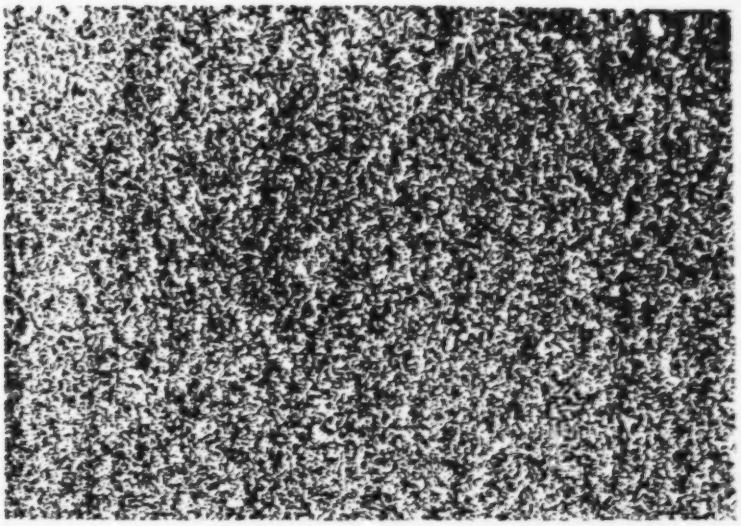

(c) weld BP102

(d) weld BP103

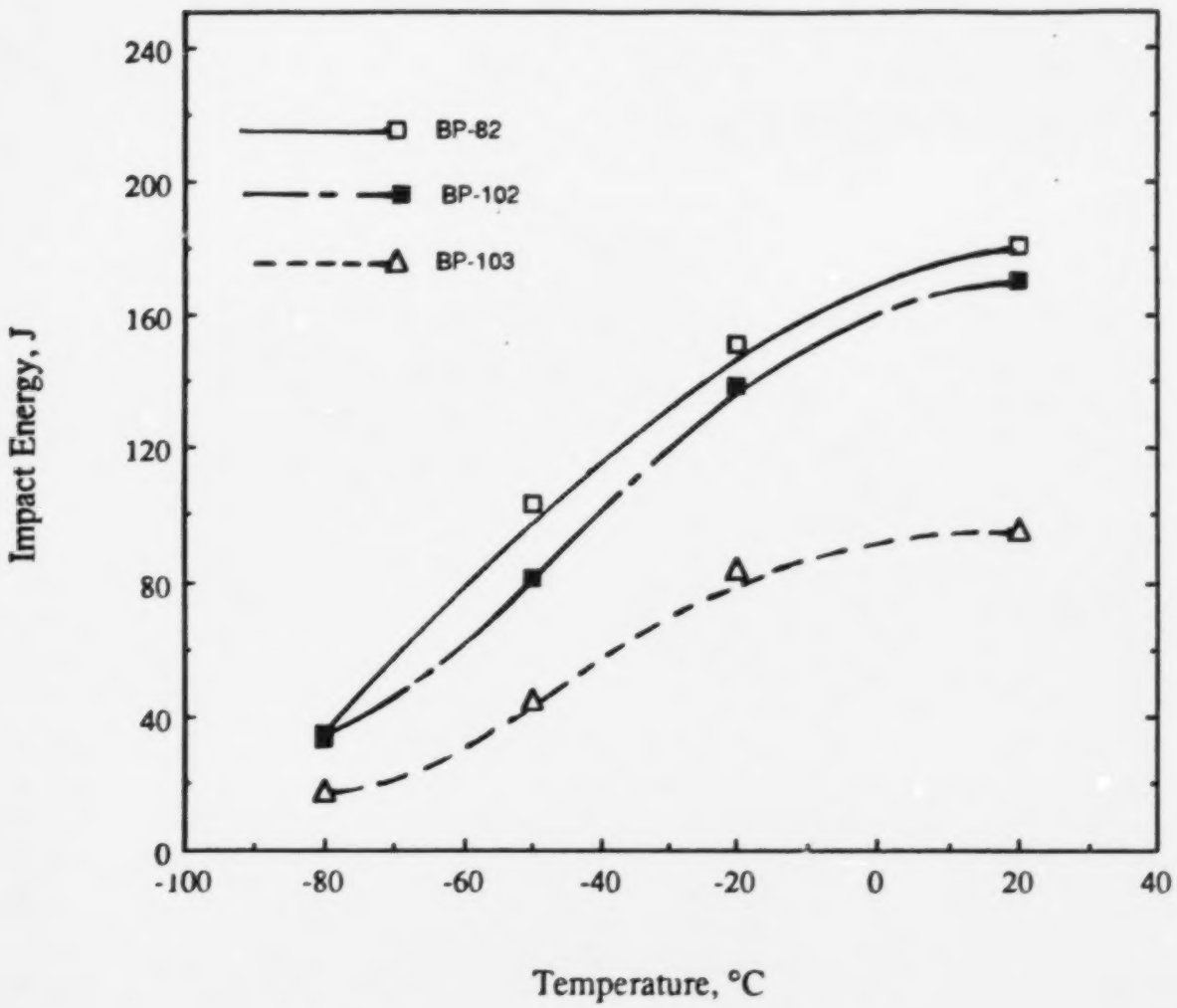

Fig. 7. Charpy transition curves of experimental rotary arc narrow gap welds.

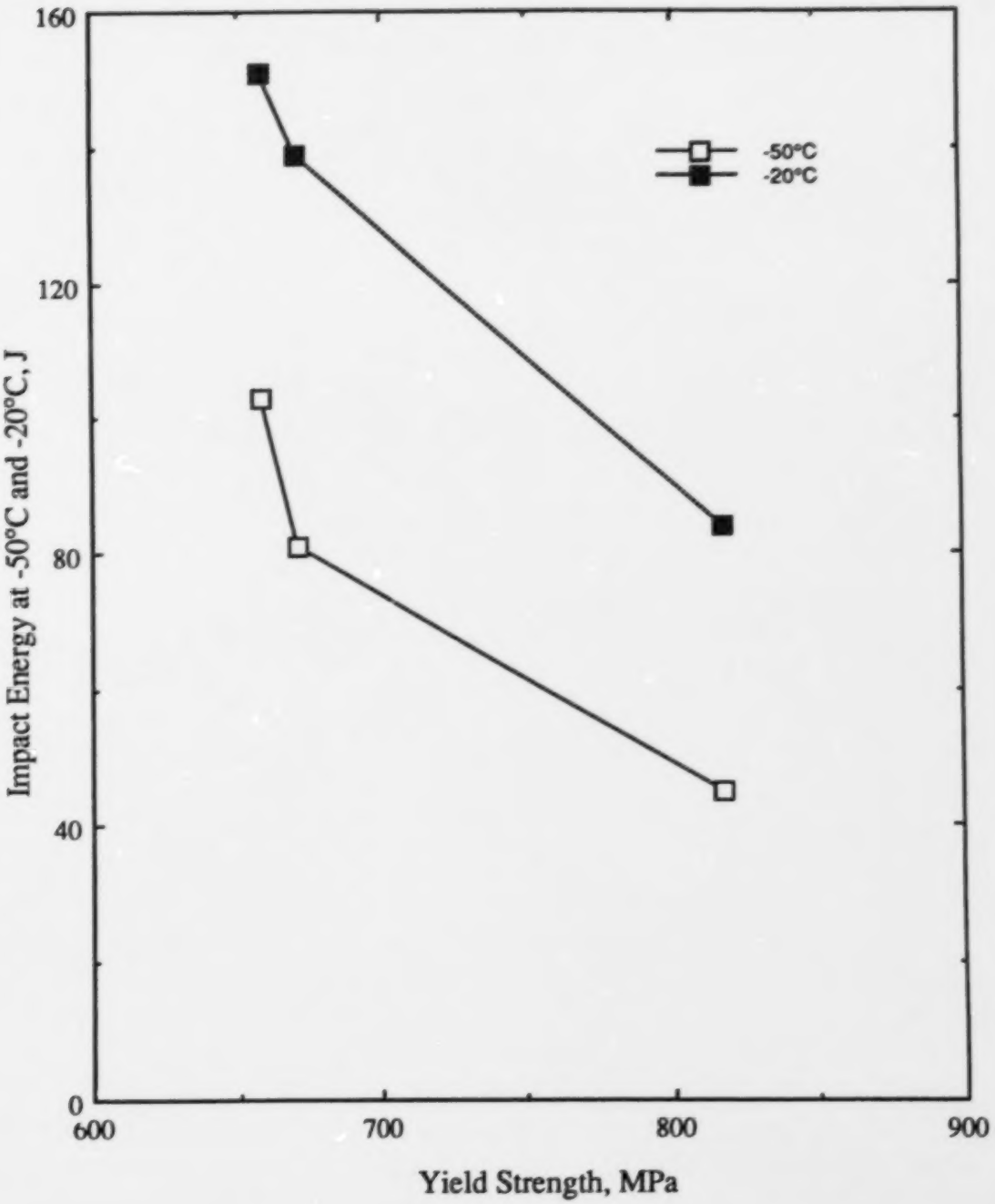

Fig. 8 Impact energy verus yield strength plot for rotary arc narrow gap welds.